Appl Biochem Biotechnol (2011) 165:1725–1739
DOI 10.1007/s12010-011-9390-0

Metabolic Flux Analysis and Principal Nodes Identification for Daptomycin Production Improvement by *Streptomyces roseosporus*

Di Huang · Xiaoqiang Jia · Jianping Wen · Guoying Wang · Guanghai Yu · Qinggele Caiyin · Yunlin Chen

Received: 21 May 2011 / Accepted: 12 September 2011 /
Published online: 30 September 2011

Abstract In the present work, a comprehensive metabolic network of *Streptomyces roseosporus* LC-54-20 was proposed for daptomycin production. The analysis of extracellular metabolites throughout the batch fermentation was evaluated in addition to daptomycin and biomass production. Metabolic flux distributions were based on stoichiometrical reaction as well as the extracellular metabolites fluxes. Experimental and calculated values for both the specific growth rate and daptomycin production rate indicated that the in silico model proved a powerful tool to analyze the metabolic behaviors based on the analysis under different initial glucose concentrations throughout the fermentation. Through manipulating different pH values, the production rates of various extracellular metabolites were also presented in this paper. Flux distribution variations revealed that the daptomycin production could be significantly influenced by the branch points of glucose 6-phosphate, 3-phosphoglycerate, phosphoenolpyruvate, pyruvate, and oxaloacetate. The five principal metabolites were certified as the flexible nodes and could form potential bottlenecks for a further enhancement of daptomycin production. Furthermore, various concentrations of the five precursors were added into the batch fermentation and led to the enhancement of daptomycin concentration and production rate.

Keywords Daptomycin production · *Streptomyces roseosporus* · Initial glucose concentrations · pH control · Metabolic flux analysis · Principal nodes identification · Precursor feeds · Batch fermentation

Electronic supplementary material The online version of this article (doi:10.1007/s12010-011-9390-0) contains supplementary material, which is available to authorized users.

D. Huang · X. Jia · J. Wen · G. Wang · G. Yu · Q. Caiyin
Department of Biochemical Engineering, School of Chemical Engineering and Technology, Tianjin University, Tianjin 300072, People's Republic of China

X. Jia · J. Wen (✉) · Q. Caiyin
Key Laboratory of Systems Bioengineering (Tianjin University), Ministry of Education, Tianjin 300072, People's Republic of China
e-mail: jpwen@tju.edu.cn

Y. Chen
School of Science, Beijing Jiaotong University, Beijing 100044, People's Republic of China

Introduction

Daptomycin is an important clinical semi-synthetic derivative of the A21978C cyclic lipopeptide antibiotics produced by *Streptomyces roseosporus* [1, 2]. Acidic lipopeptide antibiotics represent a new class of therapeutic agents that include compounds with a unique mechanism of action, such as calcium-dependent antibiotics [3], friulimicin [4], A54145 [5], and laspartomycin [6]. Structurally, daptomycin is a depsipeptide containing 13 amino acids in addition to a decanoyl fatty acid attached to the N terminus. It contains two D-configured as well as nonproteinogenic residues, L-kynurenine, L-ornithine, and L-3-methylglutamate [7]. With the particular structure, daptomycin binds to the cell membrane of Gram-positive bacteria via its lipid moiety, followed by calcium-dependent insertion and oligomerization.

The cost reduction and production improvement of the high-value secondary metabolites are hampered by their poor production. Therefore, various disciplines such as genetics, physiology, and biochemistry have been carried out to enhance the production of the secondary metabolites, especially of the antibiotics. Due to the heavy and tedious traditional work for strain screening, it is necessary to explore time- and labor-saving approaches for production improvement. Constraints-based metabolic flux analysis (MFA) is one of the most popular computational methods for predicting engineered gene targets rationally [8, 9], which is based on a stoichiometric metabolic model that represents the mass balance information of metabolites in all cellular reactions. MFA has become a powerful tool to characterize physiological states of cells via the estimation of their intracellular metabolic fluxes [10–12], by which rational changes can be introduced into the carbon metabolism so as to increase the fluxes of precursors and cofactors of antibiotics [13, 14].

Daptomycin yield has been greatly improved through the fermentation control [15]. However, attempts to build a systematical metabolic dynamics model are impeded owing to the lack of a full understanding of critical enzymes in the particular cell. Fortunately, the problems can be solved by MFA via the investigation of the intracellular behavior, phenotype, and the operational mode of metabolism, which is essential for quantitative study [16, 17]. Besides, MFA also provides significant aspects about the complex metabolic mechanism, product yield optimization, the bottlenecks in the overproduction of the desired product, and the energetic parameters identification [18–21]. Furthermore, with the aid of MFA, the effective identification of principal nodes has become a research hot spot in recent years [22–24]. Therefore, MFA plays an important role in rational design of daptomycin metabolic network. However, to date, little attempt has been made to understand quantitatively the production of daptomycin by *S. roseosporus* using the MFA method.

In the present work, the aim was to estimate the maximum daptomycin yield and to elucidate the carbon metabolic pathways leading to the high daptomycin yield. For this purpose, the batch fermentations under various conditions as well as quantitative measurement of major fermentation products were carried out. Besides an in silico constitutive network structure of cellular metabolism was established. Then, the flux distribution of the intracellular reaction network was obtained by linear optimization program. Five primary precursor metabolites through the carbon metabolism were identified as the main bottlenecks linking the primary and the secondary metabolism by flux discrepancies analysis under different pH conditions. Based on the results of rigidity for five principal nodes, a precursor supply strategy was successfully utilized to enhance the daptomycin yield.

Materials and Methods

Microorganism, Inoculum Preparation

S. roseosporus LC-54-20 was a high-daptomycin production strain, which was obtained by mutation treatment of the wild strain *S. roseosporus* NRRL 11379 stocked in our laboratory. A spore stock suspension of approximately 5×10^7 spores/mL was inoculated into 50 mL seed medium containing (per liter) 10.0 g glucose, 15.0 g starch, 5.0 g soya peptone, 5.0 g casein, 4.5 g $(NH_4)_2SO_4$, 2.0 g KH_2PO_4, 1.0 g $MgSO_4{\cdot}7H_2O$, 46.0 g 3-*N*-morpholinepropanesulfonic acid (MOPS), and 3 mL trace metal solution, in a 250-mL baffled shake-flask. Trace metal solution consisted of (per liter) 8.0 g $FeSO_4{\cdot}7H_2O$, 0.4 g $CuSO_4{\cdot}5H_2O$, 0.44 g $ZnSO_4{\cdot}7H_2O$, 0.15 g $MnSO_4{\cdot}H_2O$, 0.01 g $Na_2MoO_4{\cdot}2H_2O$, 0.02 g $CoCl_2{\cdot}2H_2O$.

Batch Fermentation

After incubation at 30 °C and 200 rpm for 48 h, seed medium was centrifuged (3,000×*g*, 5 min at 15 °C). The mycelium was washed twice with the deionized water and inoculated into the fermentation medium. The chemically defined medium contained (per liter) 15.0 g $(NH_4)_2SO_4$, 2.0 g KH_2PO_4, 1.0 g $MgSO_4{\cdot}7H_2O$, 46.0 g MOPS, and 3 mL trace metal solution. Batch fermentation was performed at 30 °C in a 7.5-L BIOFLO 110 bioreactor (NBS, USA) with an initial culture volume of 4 L. The aeration rate was controlled at 1 vvm through a hydrophobic 0.22-μm (Millipore) membrane filter. Dissolved oxygen was maintained above 20% by automatically adjusting the agitation speed from approximately 300 to 700 rpm. Antifoam (Sigma 204) was added to prevent excessive foaming. To supplement precursor, aqueous solution containing decanoic acid/ammonia (1:1, *v/v*) was added at the rate of 0.1 mL/(L h) after 48 h. The initial glucose concentration was set up in a range of 20–40 g/L. The pH was controlled at 6.5, 7.5, and 8.5 by 2 M NaOH or 2 M HCl.

Analytical Methods

Biomass Determination

For biomass measurement, 10-mL culture samples were centrifuged (3,000×*g*) and filtered through 0.22-μm nitrocellulose filter (Millipore) under vacuum. The mycelium on the filter was washed twice and then dried to a constant weight.

Analysis of Filtrate Samples

The supernatant from the above centrifugation was filtered by the same method. Both the filtrates were combined for further analysis. Glucose concentration was determined by a glucose biosensor analyzer (SBA-40C, China) as with previous work [25]. Low-molecular-weight organic acids were analyzed using a reversed-phase high-performance liquid chromatography system (Agilent 1,200, USA) with an Aminex HPX-87H ion exclusion column (300×7.8 mm, Bio-Rad Laboratories, Hercules, CA, USA) [26]. Daptomycin was determined by the improved method of Miao et al. [27] with an Extend-C18 column (250×4.6 mm, Agilent, USA). The mobile phase was 0.1% trifluoroacetic acid in water and acetonitrile (60:40, *v/v*). The flow rate was 0.8 mL/min, and the detection wavelength was

220 nm. Decanoic acid in the culture broth was analyzed by gas chromatography (Kechuang 9800, China) as described by Yu et al. [28]. The concentrations of O_2 and CO_2 were measured using EX-2,000 off-gas monitor (NBS, USA).

Precursor Feeds

Various concentrations of gluconate (10 and 20 mmol/L), serine (20 and 40 mmol/L), chorismate (8.6 and 17.2 mmol/L), alanine (20 and 40 mmol/L), aspartate (15 and 30 mmol/L), glutamate (12 and 24 mmol/L), and tryptophan (5.5 and 11 mmol/L) were added into the medium at the beginning of the fermentation. In particular, the carbons of these compounds were adjusted equivalent quantity to maintain the same molar carbons in each system.

In Silico Model Construction and Metabolic Flux Analysis

A brief description of the stoichiometric model was given below. The following major assumptions were introduced in the model:

1. All the cells performed identically throughout the fermentation.
2. Organic acid excretion and transportation processes proceeded via passive transport.
3. The genetic structure, genetic control mechanisms, and the regulation of the intracellular network of the *S. roseosporus* directed toward the target daptomycin in response to the designed environment.
4. The transcription and translation steps for daptomycin synthesis and secretion were non-limiting.
5. The mutant strain possessed the identical metabolic pathway with the genome-model strain.

The constructed network includes Embden–Meyerhof–Parnas pathway (EMP) and pentose phosphate pathway (PPP), tricarboxylic acid cycle (TCA), amino acids biosynthesis, cell growth, daptomycin formation, and other pathway reactions. The detailed reactions and corresponding abbreviations are given in Electronic Supplementary Material A and Electronic Supplementary Material B.

The theory about MFA was expounded by a previous report [16, 17]. In this model, the number of reactions was greater than the number of metabolites, and the number of unknown fluxes was greater than the number of balance equations. Then, in silico MFA model was solved by optimizing a defined objective function, such as the specific growth rate or specific product rate [18, 22]. When the specific growth rate was selected as the objective function, the specific rates for glucose uptake and the production of various extracellular metabolites (lactate, acetate, succinate, pyruvate, citrate, and α-ketoglutarate, daptomycin), which were measured during batch fermentation, were used as the constraints for model solution. When the specific daptomycin production rate was selected as the objective function, experimental specific growth rates and specific glucose uptake rate as well as organic acids were used as the constraints for calculation.

The underdetermined set of linear equations resulting from metabolic flux balancing is solved by linear optimization using Matlab 7.7.0 (MathWorks, Natick, MA, USA) [29]. It should be noted that, although the optimized value of the objective function is unique, the flux distribution may have many options. In this case, more biological or operational constraints addition could result in a unique flux distribution [30]. Furthermore, through constraining the fluxes obtained by the objective, minimizing and maximizing each flux separately, the calculated fluxes are indeed unique.

Reproducibility and Replication of Experiments

Experiments were carried out in triplicate to ensure that the trends and relationships observed in the culture parameters measured were reproducible.

Results and Discussion

Fermentation Profiles and Carbon Balance Close

The typical batch fermentation of *S. roseosporus* is shown in Fig. 1, which displays the concentration profiles of glucose, biomass, daptomycin, and organic acids throughout the course of the fermentation when initial glucose concentration was 40 g/L and pH was controlled at 7.5. Figure 1a shows that glucose was consumed at a high rate during 40–60 h.

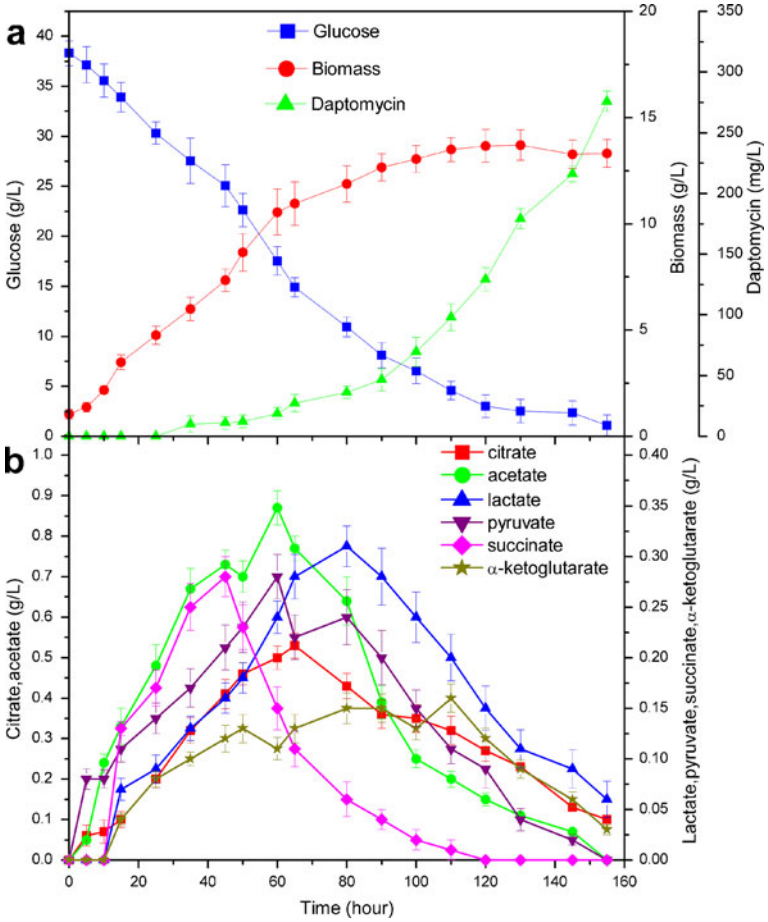

Fig. 1 Glucose, biomass dry weight, daptomycin (**a**), and organic acids (**b**) profiles during the batch fermentation process of *S. roseosporus*. Fermentation was carried out when the initial concentrations of glucose was 40 g/L, pH was 7.5

It was noticed that no obvious lag phase was observed in spite of using semi-defined medium in the inoculum and defined medium in the bioreactor. Broadly, the phenomenon was probably due to three reasons. Firstly, the inoculation volume was 10% of medium volume for the bioreactor rather than 5%, contributing to enough initial biomass concentration of the reactor (1.2 g/L). Secondly, as the adopted inocula at the exponential stage possessed higher metabolic activity, they could adapt to the new environment quickly. In addition, the chemically defined medium had been optimized to ensure the best growth and the antibiotic formation for *S. roseosporus*. In Fig. 1a, the biomass accumulated and reached to a maximum value of 13.7 g/L at 130 h, whereas daptomycin began to increase sharply from late exponential phase (approximately 100 h) with the highest concentration of 272 mg/L. To some degree, the production of organic acids presented the similar tendency (Fig. 1b), which arrived at their peaks between 40 and 110 h. After the peak, the acids were reused rapidly to exhaustion at a point coinciding with the end of stationary phase, indicating that organic acids were considered as a carbon source for cell growth. Although a detailed mechanism of organic acids formation in aerobic cultures remained unknown, different hypotheses had been suggested by *Escherichia coli* and *Streptomyces lividans* under carbon-overflow conditions [29, 31]. Organic acids formation was attributed either to limitations in respiratory NADH turnover and concomitant ATP generation through oxidative phosphorylation or to limitations in the TCA cycle. Furthermore, it could be inferred that the limitations might cause a reorganization of the catabolic flux distribution to meet the anabolic demands under different conditions by generating the necessary amount of energy through both oxidative metabolism and organic acids formation.

As the precursor, decanoic acid was added to incorporate into the daptomycin molecular structure. In fact, we manipulated the experiment at the carbon (glucose or the other substrates) metabolism level, and the decanoic acid was supplemented into the medium to enhance the cellular utilization of the fatty acid. However, decanoic acid was fed at a low level (trace quantity), thus decanoic acid metabolism was assumed to be negligible compared with the main carbon source glucose.

It is well known that carbon balance close is the prerequisite for metabolic flux analysis. As shown in Table 1, the carbon balance was satisfactory as the estimated carbon recoveries against the initial carbon input were at a range of 94.13–100.64%. At 25 h, the carbon distributions were mainly focused on acetate, CO_2, and biomass. In late exponential stage, citrate and acetate were also detected at a high concentration. However, at the end of fermentation, biomass, CO_2, and daptomycin were the main metabolites of carbon distribution without any acids detection. In addition, the maximum production rate for daptomycin occurred in late exponential phase, in which secondary metabolites biosynthesis was the optimal. Thus, the carbon recovery could prompt us to use the data during this phase for further metabolic flux calculations.

In Silico Model Construction and Verification

For the batch fermentation, glucose concentration was varied from 20 to 40 g/L. Eight specific-rates data (one for glucose consumption rate and seven for metabolites production rate) were measured during exponential growth phase of batch fermentation. It was observed that with the increase in initial glucose concentrations, the daptomycin production rate increased from 1.03×10^{-2} to 1.46×10^{-2} and then decreased to 5.23×10^{-3} mmol/g DCW/h. Interestingly, the uptake profiles of other metabolites appeared to be complicated (Table 2). When initial glucose concentration attained 30 g/L, lactate consumption rate increased to the highest, and citrate consumption decreased to the lowest. For the initial

Table 1 Carbon mass balance for daptomycin fermentation by *S. roseosporus*

Time (h)[a]	Carbon mass (mol/L)[b]											
	Glucose	Biomass[c]	Citrate	Acetate	Lactate	Pyruvate	Succinate	α-Ketoglutarate	CO_2[d]	Daptomycin	Total carbon	Carbon balance (%)[e]
0	1.277	0.040	0.000	0.000	0.000	0.000	0.000	0.000	0.000	0.000	1.317	100.00
5	1.238	0.052	0.002	0.002	0.000	0.003	0.000	0.000	0.014	0.000	1.310	99.50
15	1.131	0.133	0.003	0.011	0.002	0.004	0.004	0.001	0.035	0.000	1.325	100.64
25	1.010	0.180	0.006	0.016	0.003	0.005	0.006	0.003	0.053	0.000	1.283	97.42
35	0.918	0.228	0.010	0.022	0.004	0.006	0.008	0.003	0.065	0.000	1.265	96.10
45	0.836	0.279	0.013	0.024	0.005	0.007	0.009	0.004	0.101	0.000	1.279	97.18
60	0.585	0.401	0.016	0.029	0.008	0.010	0.005	0.004	0.182	0.001	1.239	94.13
65	0.497	0.416	0.017	0.026	0.009	0.007	0.004	0.004	0.280	0.001	1.262	95.83
80	0.365	0.451	0.013	0.021	0.010	0.008	0.002	0.005	0.370	0.002	1.248	94.78
100	0.218	0.496	0.011	0.008	0.008	0.005	0.001	0.004	0.507	0.003	1.262	95.83
120	0.100	0.519	0.008	0.005	0.005	0.003	0.000	0.004	0.599	0.006	1.250	94.91
145	0.078	0.504	0.004	0.002	0.003	0.001	0.000	0.002	0.644	0.010	1.248	94.81

[a] The initial glucose concentration was 40 g/L

[b] It was assumed that the carbon from inoculum was negligible. Each value was an average from three different independent experiments

[c] It was assumed that the average composition of *S. roseosporus* biomass was $CH_{1.81}O_{0.58}N_{0.2}S_{0.004}P_{0.01}$ and its composition was kept constant during the fermentation [14]

[d] CO_2 in the liquid phase was ignored

[e] Calculated based on initial total carbon mass

Table 2 Experimental metabolic rates and constraints for different initial glucose concentrations used by in silico MFA

Specific uptake/production rate (mmol/g DCW/h)	Initial glucose (g/L)					
	20		30		40	
	Experimental[a]	In silico[b]	Experimental	In silico	Experimental	In silico
Glucose	$-(0.733\pm0.124)$		$-(0.425\pm0.111)$		$-(0.258\pm0.051)$	
Citrate	$-(0.79\pm0.33)\times10^{-3}$		$-(0.66\pm0.43)\times10^{-3}$		$-(1.14\pm0.51)\times10^{-3}$	
Acetate	$-(1.79\pm0.27)\times10^{-2}$		$-(4.40\pm0.15)\times10^{-2}$		$-(7.21\pm0.30)\times10^{-2}$	
Lactate	$-(1.89\pm0.22)\times10^{-2}$	–	$-(2.37\pm0.18)\times10^{-2}$	–	$-(1.32\pm0.15)\times10^{-2}$	–
Pyruvate	$-(2.15\pm0.22)\times10^{-2}$		$-(5.31\pm0.21)\times10^{-3}$		$-(6.68\pm0.33)\times10^{-3}$	
Succinate	Not detected		$-(2.34\pm0.75)\times10^{-3}$		$-(3.73\pm0.51)\times10^{-3}$	
α-Ketoglutarate	Not detected		$-(3.46\pm0.38)\times10^{-3}$		$-(0.75\pm0.36)\times10^{-3}$	
Daptomycin	$(1.41\pm0.34)\times10^{-2}$	1.87×10^{-2}	$(3.21\pm0.72)\times10^{-2}$	3.82×10^{-2}	$(1.05\pm0.28)\times10^{-2}$	1.36×10^{-2}
Specific growth rate (h^{-1})	0.038 ± 0.015	0.049	0.017 ± 0.006	0.023	0.012 ± 0.005	0.015

Plus-minus sign production, *minus sign* uptake

[a] Measured during late exponential growth phase of batch fermentation (50–60 h for 20 g glucose/L, 65–75 h for 30 g glucose/L, and 90–100 h for 40 g glucose/L) and used as the constraints in the model

[b] For the daptomycin production rate calculation, the specific growth rate was used as an objective function; for the specific growth rate, the specific daptomycin production rate was used as an objective function for MFA

glucose concentration of 40 g/L, the specific consumption rate of acetate, pyruvate, and succinate reached the highest levels among initial glucose concentrations.

Specific growth rate and specific daptomycin production rate were used as the objective function, respectively, and experimental values were used as the criterion to evaluate the agreement between the in silico MFA and the experimental. For all three cases of glucose concentrations, differences between the in silico MFA and experiments were observed for the specific growth rate and daptomycin production rate. The maximum specific growth rate was about 1.3 times higher than those values measured from the experiment. One reason resulted in the discrepancy might be the biomass formation equation obtained from the cellular composition of *Streptomyces coelicolor*, rather than from *S. roseosporus*, which was unavailable from the literature. Another reason is that the constructed metabolic network was simplified by deleting some branch reactions which were not adjacent to the central carbon metabolism, and thus generated some discrepancy. When specific daptomycin production rate was selected as the objective function, the observed daptomycin production rate was 0.3×10^{-2}–0.5×10^{-2} mmol/g DCW/h less than the optimum. Naeimpoor and Mavituna also explained the differences between the experimental and calculated values, mainly resulted from the constrained carbon distribution by the experimental specific oxygen uptake, carbon dioxide, and actinorhodin production rates [32]. Unlike organic acids and amino acids, the biosynthesis of antibiotics was much more complex. Here, the detailed synthetic pathway was only illustrated in an overall reaction. Besides, the transcription and translation steps for daptomycin synthesis and secretion were considered non-limiting. Therefore, it is difficult to simulate the actual value in a clear way. Although the results obtained in the experiments guided by the constructed network model were not as well as the predicted after excluding some reactions, this model could still solve the underdetermined system with known rates, which was useful especially when the in

vivo rates were hard to quantify. Therefore, the metabolic flux distribution of *S. roseosporus* fermentation could be analyzed by the constructed network model.

Metabolic Flux Analysis for Different Initial Glucose Concentrations

Metabolic flux of *S. roseosporus* during daptomycin fermentation was analyzed by the metabolic network. Table 3 shows the carbon flux distribution at the same phase of the fermentation with different initial glucose concentrations. All fluxes are normalized as a percentage of the glucose uptake rate. The flux of reaction catalyzed by phosphoglucose isomerase was twofold higher than that of glucose-6-phosphate dehydrogenase. The reaction catalyzed by pyruvate kinase presented a higher activity with increasing initial

Table 3 Metabolic flux distributions of central carbon metabolism for different initial glucose concentrations during the late exponential stage of batch culture

Reaction	Enzyme	Initial glucose (g/L)		
		20	30	40
EMP				
R1	Hexokinase	100	100	100
R2	Phosphoglucose isomerase	68	73	71
R3	Phosphofructokinase/fructose bisphosphate aldolase	79	75	75
R4	Triose phosphate isomerase	82	82	82
R5	Glyceraldehyde-3-phosphate dehydrogenase/phosphoglycerate kinase	165	169	163
R6	Phosphoglycerate phosphomutase/enolase	142	137	147
R7	Pyruvate kinase	78	70	83
TCA cycle				
R21	Citrate synthase	55	60	55
R22	Aconitase A	57	59	56
R23	Isocitrate dehydrogenase	57	59	56
R24	α-Ketoglutarate dehydrogenase	52	50	51
R25	Succinic thiokinase	48	49	54
R26	Succinate dehydrogenase	53	50	51
R27	Fumarase	68	67	67
R28	Malate dehydrogenase	35	38	42
PPP				
R8	Glucose-6-phosphate dehydrogenase	32	27	29
R9	Ribose-5-phosphate isomerase	21	20	19
R10	Ribose-5-phosphate epimerase	13	14	16
R11	Transketolase	8	9	10
R12	Transketolase	7	7	8
R13	Transaldolase	8	9	10
Anaplerotic pathway				
R18	PEP carboxylase	63	66	64
R19	Pyruvate carboxylase	0	0	0
R20	Malic enzyme	33	29	25

The given values correspond to fluxes calculated by maximization of specific growth rate

glucose concentration, which enhanced the flux toward pyruvate and related over-flow metabolites of the TCA cycle. The flux into EMP was much higher than the demand for the PPP. This flux distribution revealed that glucose was mainly directed to pyruvate via the EMP. The different demand for NADPH led to various flux distributions through the PPP. The relative flux distribution through the PPP depended on the initial glucose concentrations, ranging from 27% to 32% (Table 3). The differences were apparently due to the increase of amino acid synthesis for daptomycin production. In TCA cycle, the fluxes of reaction catalyzed by succinate dehydrogenase and malate dehydrogenase did not change significantly. In particular, TCA flux was high (approximate 60%) enough to supply the NADPH cofactor and other intermediate precursors. For anaplerotic pathway, the fluxes from phosphoenolpyruvate (PEP) ranged between 63% and 66%. Oxaloacetate (OA) supplied by R18 (R19=0) was required more (66%) at 30 g/L initial glucose condition.

Principal Nodes Identification with Different pH Control

In order to investigate the effect of pH on the metabolic flux distribution, the batch fermentations were carried out under different pH conditions (6.5, 7.5, and 8.5). The accumulation rates obtained from experiments for glucose uptake, organic acids formation, and biomass formation are listed in Table 4.

It was noted that the highest daptomycin production rate of 0.017 mmol/g DCW/h was obtained at pH 7.5. The condition of pH 7.5 also resulted in the highest value in glucose, citrate, acetate, and α-ketoglutarate uptake rate. It could be concluded that these organic acids were utilized as the carbon source while the production of daptomycin was preferable for a higher value. The specific growth rate was almost the same under pH 6.5 and 7.5, indicating little discrepancy. Furthermore, the pH level was considered as an indicator for evaluating the efficiency of daptomycin production during glucose fermentation (Table 4).

Like the case of different glucose concentrations, the similar conclusion was obtained between the EMP and PPP fluxes under different pH conditions (data not shown). Metabolic flux distributions revealed that growth and product formation on these conditions not only led to dramatic flux changes through the metabolic pathways but also contributed

Table 4 Experimental metabolic rates and constraints for different pH conditions used by in silico MFA

Specific uptake/production rate (mmol/g DCW/h)	pH[a]		
	6.5	7.5	8.5
Glucose	–(0.337±0.103)	–(0.425±0.111)	–(0.343±0.090)
Citrate	$-(0.66\pm0.63)\times10^{-3}$	$-(0.86\pm0.43)\times10^{-3}$	$-(0.59\pm0.39)\times10^{-3}$
Acetate	$-(3.40\pm0.35)\times10^{-2}$	$-(4.40\pm0.15)\times10^{-2}$	$-(3.89\pm0.44)\times10^{-2}$
Lactate	$-(3.73\pm0.35)\times10^{-2}$	$-(2.37\pm0.18)\times10^{-2}$	$-(2.09\pm0.26)\times10^{-2}$
Pyruvate	$-(6.66\pm0.34)\times10^{-3}$	$-(5.31\pm0.21)\times10^{-3}$	$-(3.63\pm0.36)\times10^{-3}$
Succinate	$-(1.78\pm0.67)\times10^{-3}$	$-(2.34\pm0.75)\times10^{-3}$	$-(4.32\pm0.55)\times10^{-3}$
α-Ketoglutarate	$-(1.88\pm0.28)\times10^{-3}$	$-(3.46\pm0.38)\times10^{-3}$	$-(1.06\pm0.25)\times10^{-3}$
Specific growth rate (h^{-1})	$(3.05\pm0.59)\times10^{-2}$	$(3.21\pm0.72)\times10^{-2}$	$(2.67\pm0.86)\times10^{-2}$
Daptomycin	0.013±0.005	0.017±0.006	0.010±0.006

Plus-minus sign production, *minus sign* uptake

[a] Measured during late exponential growth phase (65–75 h) of batch fermentation (initial glucose was 30 g/L) and used as the constraints in the model

to significant changes in flux partitioning around the principal nodes for product formation [33, 34]. Therefore, it is necessary to estimate the fluxes through the metabolic pathways under different pH conditions, and thus to explore the rigidity of these principal nodes for daptomycin over-production.

There are 12 precursor metabolites from which all chemicals can be biosynthesized through the carbon metabolism [35]. The normalization was performed by assigning 100% to the flux for the reactions R1, R5, R6, R7, and R18, respectively, and calculating the other fluxes accordingly. Therefore, all incoming fluxes to a node equaled all outgoing fluxes from a node. The calculated fluxes around the five principal nodes (glucose 6-phosphate (G6P), 3-phospho-glycerate (3PG), PEP, pyruvate (Pyr), and OA) under different pH conditions are illustrated in Fig. 2.

Figure 2a shows the different flux distributions around the G6P branch node under different pH conditions. The results indicated that the fraction of the carbon from G6P to RL5P was between 17% and 32% for the different pH control. At the G6P branch node, use of glucose as the carbon source resulted in different fluxes toward the PPP pathway. The fluxes around the 3PG node are presented in Fig. 2b. The fluxes via Ser to daptomycin were approximately different for three cases. In the present study, 3PG was mainly channeled to the synthesis of PEP (Fig. 2b). There was a relatively low flux to Ser synthesis during cultivations. However, when the strain was cultivated at pH 7.5, the principal node analysis on the 3PG branch showed a 1.5-fold flux increase toward Ser compared with that obtained at pH 8.5. As for the PEP, Fig. 2c reveals that the flux via chorismate to daptomycin production exhibited approximately twofold increase from pH 8.5 to 7.5, whereas the fraction of carbon flux to OA did not change significantly. It was concluded that the PEP metabolism conferred the cell flexibility to regulate the energy and intermediate fluxes under various environmental conditions. Therefore, the metabolic state was controlled by various regulators that normally adopted appropriate cellular responses to environmental signals. At the Pyr node, no acetate and lactate was formed; instead, they were consumed as the carbon sources so the direction of carbon flow to acetate and lactate was in reverse (Fig. 2d). The flux of Pyr via Ala played a key role in daptomycin yield and the flux to Ala changed in the range of 8–16%. In Fig. 2e, the flux partitions around OA node varied significantly to meet different requirements. The fraction of the flux from OA to Asp changed a lot with the increasing pH. Our results indicated that the product distribution and metabolic fluxes changed significantly with different culture environments.

The other nodes such as α-ketoglutarate (AKG), erythrose 4-phosphate (E4P) were considered as rigid nodes due to little change (data not shown). The comparisons of principal nodal split ratios among the different carbons could determine the sensitivity of these nodes to perturbations and how changes in these nodes affect daptomycin yield. Thus, considering these five nodes through the bioprocess, conditions seemed to be more favorable to obtain desirable distribution of fluxes toward daptomycin production. Large changes in flux partitioning around these five principal nodes were required for daptomycin production. As the precursors of daptomycin, the rigidity or flexibility of these nodes determined whether they were potential bottlenecks for a further increase of daptomycin production [36].

Effect of Precursor Feeds on Daptomycin Production

According to the above analysis, the daptomycin production rate was elucidated to be significantly affected by the five principal nodes. Therefore, five precursors were added to the culture under various concentrations to validate the model prediction. Besides,

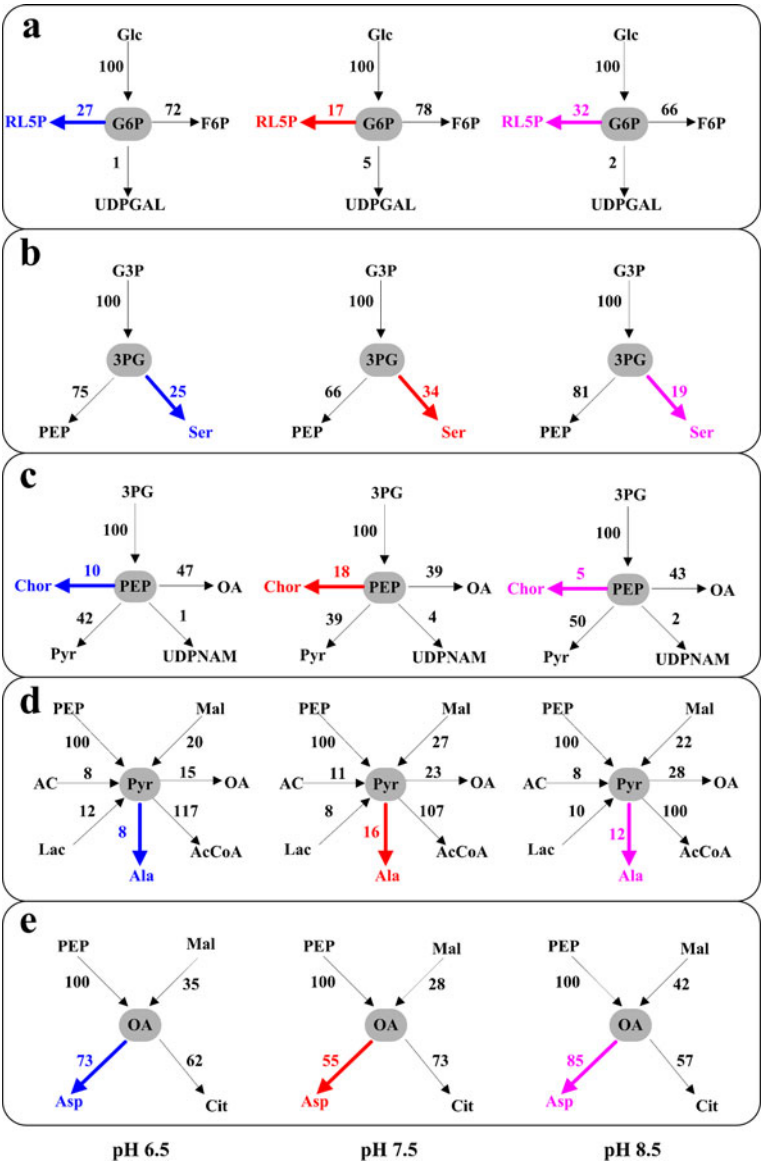

Fig. 2 Normalized metabolic flux distributions at five nodes for different pH control of batch fermentation. **a** Glucose-6-phosphate (G6P) node; **b** 3-Phosphoglycerate (3PG) node; **c** Phosphoenolpyruvate (PEP) node; **d** Pyruvate (Pyr) node; **e** Oxaloacetate (OA) node. The other abbreviations are given in the Electronic Supplementary Materials. The pH conditions were 6.5, 7.5, and 8.5, respectively

glutamate and tryptophan were fed in the medium as the negative control, as depicted in Table 5.

Compared with the glucose control groups (10 and 20 mmol/L), the daptomycin concentration and daptomycin production rate increased in the fermentative process. When 30 mmol/L aspartate was added to the fermentation medium in the flask culture, the highest daptomycin production rate (2.56 mg/g DCW/h) and the daptomycin concentration

Table 5 Characteristics of precursor addition on daptomycin production in batch fermentation

Precursors (mmol/L)[a]		Daptomycin concentration (mg/L)	Daptomycin production rate (mg/g DCW/h)	Glucose consumption rate (mg/g DCW/h)	Biomass (g/L)
Glucose	10	268±22	1.25±0.11	6.68±0.56	16.97±1.56
	20	272±20	1.27±0.10	5.77±0.55	18.25±1.45
Gluconate	10	325±24	1.87±0.14	6.94±0.63	15.69±1.59
	20	347±25	1.95±0.18	6.63±0.67	16.04±1.63
Serine	20	305±24	1.61±0.16	6.73±0.66	15.98±1.44
	40	296±22	1.54±0.16	6.79±0.62	16.23±1.63
Chorismate	8.6	342±25	1.95±0.20	6.92±0.68	16.33±1.46
	17.2	349±25	1.74±0.17	6.21±0.60	18.59±1.59
Alanine	20	299±24	1.57±0.16	6.18±0.60	17.73±1.37
	40	294±24	1.64±0.17	6.62±0.66	16.95±1.41
Aspartate	15	362±25	2.50±0.18	8.23±0.73	16.08±1.56
	30	364±21	2.56±0.19	8.20±0.73	15.89±1.63
Glutamate	12	276±19	1.23±0.10	6.73±0.53	16.66±1.33
	24	277±24	1.27±0.11	6.26±0.50	16.98±1.55
Tryptophan	5.5	256±20	1.28±0.07	6.39±0.61	16.24±1.45
	11	262±23	1.25±0.09	6.31±0.55	16.51±1.39

[a] The fermentation time was 144 h

(364 mg/L) were achieved, which was 104.8% and 33.82% higher than those of the controls (glucose 20 mmol/L), respectively. For the other precursor's experiments (gluconate, serine, chorismate, and alanine), the daptomycin concentrations were enhanced by 21.27%, 13.81%, 27.61%, and 11.57%, respectively, than the control group containing 10 mmol/L glucose as well as an increase of daptomycin production rates by 38.78%, 21.21%, 50.73%, and 31.51% correspondingly. Furthermore, for 20 mmol/L glucose group, the daptomycin concentration improvement was varied from 8.09% to 28.31%, and the increased daptomycin production rate was between 21.26% and 53.54%. These results showed that the available precursor was effective to improve the production. It was also indicated that no obvious effect on the biomass was observed for different precursor feeding strategies. On the other hand, the glucose (as the main carbon) consumption rate was significantly affected by the precursor additions. When glutamate and tryptophan were fed as the precursors, no obvious changes were found compared with the glucose group, suggesting that AKG and E4P had little influence on the daptomycin flux ratio and could not be modified as the flexible nodes.

Conclusions

As illustrated, the stoichiometric model of the daptomycin-producing *S. roseosporus* was set up and used to illustrate the complex metabolic processes including daptomycin metabolism, amino acid utilization, and simultaneous consumption of organic and glucose accurately. Fluxes obtained under various initial glucose concentrations were used to demonstrate the intracellular flux distribution and verify the model. The comparison of flux

changes for different fermentation conditions (pH) gave the better understanding of the response of daptomycin yield on environmental perturbations and determined flux split ratios at principal pathways. By taking different pH conditions in batch fermentation, five principal nodes, G6P, 3PG, PEP, Pyr, and OA, were identified as the flexible nodes, and the potential bottlenecks of daptomycin production improvement. Furthermore, it was demonstrated that the synthesis efficiency and the yield of daptomycin could be enhanced by adding five precursors in batch fermentation. Obviously, the strategy complemented conventional medium design and optimization. The carbon flux distributions of daptomycin would be the focus of future research. Besides, based on these results, the model predictions of intracellular fluxes would be very interesting for the future advances of metabolic fluxes to further improve antibiotics production.

Acknowledgments The authors wish to acknowledge the financial support provided by the National 973 Project of China (No. 2011CB710800), the Key Program of National Natural Science Foundation of China (Grant No. 20936002), National Natural Science Foundation of China (No. 21076022).

References

1. Eliopoulos, G. M. (2009). Microbiology of drugs for treating multiply drug-resistant Gram-positive bacteria. *Journal of Infection, 59*, s17–s24.
2. Nailor, M. D., & Sobel, J. D. (2009). Antibiotics for gram-positive bacterial infections: Vancomycin, teicoplanin, quinupristin/dalfopristin, oxazolidinones, daptomycin, dalbavancin, and telavancin. *Infectious Disease Clinics of North America, 23*, 965–982.
3. Hojati, Z., Milne, C., Harvey, B., Gordon, L., Borg, M., Flett, F., et al. (2002). Structure, biosynthetic origin, and engineered biosynthesis of calcium-dependent antibiotics from *Streptomyces coelicolor*. *Chemistry & Biology, 9*, 1175–1187.
4. Vertesy, L., Ehlers, E., Kogler, H., Kurz, M., Meiwes, J., Seibert, G., et al. (2000). Friulimicins: novel lipopeptide antibiotics with peptidoglycan synthesis inhibiting activity from *Actinoplanes friuliensis sp. nov.* II. Isolation and structural characterization. *The Journal of Antibiotics, 53*, 816–827.
5. Miao, V., Brost, R., Chapple, J., She, K., Gal, M. F., & Baltz, R. H. (2006). The lipopeptide antibiotic A54145 biosynthetic gene cluster from *Streptomyces fradiae*. *Journal of Industrial Microbiology and Biotechnology, 33*, 129–140.
6. Borders, D. B., Leese, R. A., Jarolmen, H., Francis, N. D., Fantini, A. A., Falla, T., et al. (2007). Laspartomycin, an acidic lipopeptide antibiotic with a unique peptide core. *Journal of Natural Products, 70*, 443–446.
7. Baltz, R. H. (2008). Biosynthesis and genetic engineering of lipopeptide antibiotics related to daptomycin. *Current Topics in Medicinal Chemistry, 8*, 618–638.
8. Alper, H., Jin, Y. S., Moxley, J. F., & Stephanopoulos, G. (2005). Identifying gene targets for the metabolic engineering of lycopene biosynthesis in *Escherichia coli*. *Metabolic Engineering, 7*, 155–164.
9. David, H., Ozçelik, I. S., Hofmann, G., & Nielsen, J. (2008). Analysis of *Aspergillus nidulans* metabolism at the genome-scale. *BMC Genomics, 9*, 163.
10. Boyle, N. R., & Morgan, J. A. (2009). Flux balance analysis of primary metabolism in *Chlamydomonas reinhardtii*. *BMC Systems Biology, 3*, 4.
11. Lee, S. J., Lee, D. Y., Kim, T. Y., Kim, B. H., Lee, J., & Lee, S. Y. (2005). Metabolic engineering of *Escherichia coli* for enhanced production of succinic acid, based on genome comparison and in silico gene knockout simulation. *Applied and Environmental Microbiology, 71*, 7880–7887.
12. Mukhopadhyay, A., Redding, A. M., Rutherford, B. J., & Keasling, J. D. (2008). Importance of systems biology in engineering microbes for biofuel production. *Current Opinion in Biotechnology, 19*, 228–234.
13. Gunnarsson, N., Eliasson, A., & Nielsen, J. (2004). Control of fluxes towards antibiotics and the role of primary metabolism in production of antibiotics. *Advances in Biochemical Engineering/Biotechnology, 88*, 137–178.
14. Borodina, I., Siebring, J., Zhang, J., Smith, C. P., van Keulen, G., Dijkhuizen, L., et al. (2008). Antibiotic overproduction in *Streptomyces coelicolor* A3(2) mediated by phosphofructokinase deletion. *The Journal of Biological Chemistry, 283*, 25186–25199.

15. Huber, F. M., Pieper, R. L., & Tietz, A. J. (1988). The formation of daptomycin by supplying decanoic acid to *Streptomyces roseosporus* cultures producing the antibiotic complex A21978C. *Journal of Biotechnology, 7*, 283–292.
16. Vallino, J. J., & Stephanopoulos, G. (1993). Metabolic flux distributions in *Corynebacterium glutamicum* during growth and lysine overproduction. *Biotechnology and Bioengineering, 41*, 633–646.
17. Vallino, J. J., & Stephanopoulos, G. (1994). Carbon flux distributions at the pyruvate branch point in *Corynebacterium glutamicum* during lysine overproduction. *Biotechnology Progress, 10*, 320–326.
18. Kim, H. B., Smith, C. P., Micklefield, J., & Mavituna, F. (2004). Metabolic flux analysis for calcium dependent antibiotic (CDA) production in *Streptomyces coelicolor*. *Metabolic Engineering, 6*, 313–325.
19. Blank, L. M., & Kuepfer, L. (2010). Metabolic flux distributions: Genetic information, computational predictions, and experimental validation. *Applied Microbiology and Biotechnology, 86*, 1243–1255.
20. Melzer, G., Dalpiaz, A., Grote, A., Kucklick, M., Göcke, Y., Jonas, R., et al. (2007). Metabolic flux analysis using stoichiometric models for *Aspergillus niger*: Comparison under glucoamylase-producing and non-producing conditions. *Journal of Biotechnology, 132*, 405–417.
21. Xu, H., Dou, W. F., Xu, H. Y., Zhang, X. M., Rao, Z. M., Shi, Z. P., et al. (2009). A two-stage oxygen supply strategy for enhanced L-arginine production by *Corynebacterium crenatum* based on metabolic fluxes analysis. *Biochemical Engineering Journal, 43*, 41–51.
22. Celik, E., Calik, P., & Oliver, S. G. (2010). Metabolic flux analysis for recombinant protein production by *Pichia pastoris* using dual carbon sources: Effects of methanol feeding rate. *Biotechnology and Bioengineering, 105*, 317–329.
23. Sauer, U., & Eikmanns, B. J. (2005). The PEP-pyruvate-oxaloacetate node as the switch point for carbon flux distribution in bacteria. *FEMS Microbiology Reviews, 29*, 765–794.
24. Gao, H. J., Du, G. C., & Chen, J. (2006). Analysis of metabolic fluxes for hyaluronic acid (HA) production by *Streptococcus zooepidemicus*. *World Journal of Microbiology and Biotechnology, 22*, 399–408.
25. Nie, Z. K., Ji, X. J., Huang, H., Du, J., Li, Z. Y., Qu, L., et al. (2011). An effective and simplified fed-batch strategy for improved 2,3-butanediol production by *Klebsiella oxytoca*. *Applied Biochemistry and Biotechnology, 163*, 946–953.
26. Ji, X. J., Huang, H., Li, S., Du, J., & Lian, M. (2008). Enhanced 2,3-butanediol production by altering the mixed acid fermentation pathway in *Klebsiella oxytoca*. *Biotechnology Letters, 30*, 731–734.
27. Miao, V., Coëffet-Legal, M. F., Brian, P., Brost, R., Penn, J., Whiting, A., et al. (2005). Daptomycin biosynthesis in *Streptomyces roseosporus*: Cloning and analysis of the gene cluster and revision of peptide stereochemistry. *Microbiology, 151*, 1507–1523.
28. Yu, G., Jia, X., Wen, J., Lu, W., Wang, G., Caiyin, Q., et al. (2011). Strain improvement of *Streptomyces roseosporus* for daptomycin production by rational screening of He-Ne laser and NTG induced mutants and kinetic modeling. *Applied Biochemistry and Biotechnology, 163*, 729–743.
29. Varma, A., & Palsson, B. O. (1994). Stoichiometric flux balance models quantitatively predict growth and metabolic by-product secretion in wild-type *Escherichia coli* W3110. *Applied and Environmental Microbiology, 60*, 3724–3731.
30. Gheshlaghi, R., Scharer, J. M., Moo-Young, M., & Douglas, P. L. (2007). Metabolic flux analysis for optimizing the specific growth rate of recombinant *Aspergillus niger*. *Bioprocess and Biosystems Engineering, 30*, 397–418.
31. Madden, T., Ward, J. M., & Ison, A. P. (1996). Organic acid excretion by *Streptomyces lividans* TK24 during growth on defined carbon and nitrogen sources. *Microbiology, 142*, 3181–3185.
32. Naeimpoor, F., & Mavituna, F. (2000). Metabolic flux analysis in *Streptomyces coelicolor* under various nutrient limitations. *Metabolic Engineering, 2*, 140–148.
33. Pons, A., Dussap, C. G., Péquignot, C., & Gros, J. B. (1996). Metabolic flux distribution in *Corynebacterium melassecola* ATCC 17965 for various carbon sources. *Biotechnology and Bioengineering, 51*, 177–189.
34. Fürch, T., Wittmann, C., Wang, W., Franco-Lara, E., Jahn, D., & Deckwer, W. D. (2007). Effect of different carbon sources on central metabolic fluxes and the recombinant production of a hydrolase from *Thermobifida fusca* in *Bacillus megaterium*. *Journal of Biotechnology, 132*, 385–394.
35. Rokem, J. S., Lantz, A. E., & Nielsen, J. (2007). Systems biology of antibiotic production by microorganisms. *Natural Product Reports, 24*, 1262–1287.
36. van Gulik, W. M., de Laat, W. T., Vinke, J. L., & Heijnen, J. J. (2000). Application of metabolic flux analysis for the identification of metabolic bottlenecks in the biosynthesis of penicillin-G. *Biotechnology and Bioengineering, 68*, 602–618.